Int. J. Mol. Sci. **2004**, *5*, 333-346

International Journal of
Molecular Sciences
ISSN 1422-0067
© 2004 by MDPI
www.mdpi.org/ijms/

Calculated Electronic Behavior and Spectrum of $Mg^+@C_{60}$ Using a Simple Jellium-shell Model

W. Even [1], J. Smith [2], M.W. Roth [3,*] and H.A. Schuessler [4]

[1] Present address: Department of Physics and Astronomy, Louisiana State University, Baton Rouge, LA 70803-4001, U.S.A.
[2] Present address: Department of Aeronautics and Astronautics Engineering, Purdue University, West Lafayette, IN 47907, U.S.A.
[3] Department of Physics, University of Northern Iowa, Cedar Falls, IA 50614, U.S.A.
[4] Department of Physics, Texas A&M University, College Station, TX 77843-4242, U.S.A.

* Author to whom correspondence should be addressed; URL: http://www.physics.uni.edu/roth.shtml; E-mail: rothm@uni.edu; Tel.: (+1) 319.273.7336; Fax: (+1) 319.273.7136

Received: 23 July 2004 / Accepted: 15 November 2004 / Published: 30 November 2004

Abstract: We present a method for calculating the energy levels and wave functions of any atom or ion with a single valence electron encapsulated in a Fullerene cage using a jelluim-shell model. The valence electron-core interaction is represented by a one-body pseudo-potential obtained through density functional theory with strikingly accurate parameters for Mg^+ and which reduces to a purely Coulombic interaction in the case of H. We find that most energy states are affected little by encapsulation. However, when either the electron in the non-encapsulated species has a high probability of being near the jellium cage, or when the cage induces a maximum electron probability density within it, the energy levels shift considerably. Mg^+ shows behavior similar to that of H, but since its wave functions are broader, the changes in its energy levels from encapsulation are slightly more pronounced. Agreement with other computational work as well as experiment is excellent and the method presented here is generalizable to any encapsulated species where a one-body electronic pseudo-potential for the free atom (or ion) is available. Results are also presented for off-center hydrogen, where a ground state energy minimum of -14.01 eV is found at a nuclear displacement of around 0.1 Å.

Keywords: Encapsulation, confined atoms, magnesium, Fullerenes, spectral shift.

Introduction

The quantum mechanical behavior of hydrogen and hydrogen-like (hydrogenic) atoms is well understood and is standard regimen in introductory quantum mechanics texts [1-3]. Since the early part of the last century the behavior of *confined* atoms has been of interest. Early analytical results for hydrogen confined within a non-interacting impenetrable spherical cavity [4,5] (with infinite potential outside the sphere so the wave function vanishes on its surface) showed that as the size of the confining sphere lessens the energy levels raise, and there ultimately comes a point where the electron becomes delocalized, behaving somewhat like a particle in a sphere [5]. Although of general theoretical interest, such calculations had little practical importance until the relatively recent discovery of Fullerenes [6] and other structures capable of quantum confinement of atoms, that is, localizing atoms such that their electronic states are considerably altered.

Obviously a non-interacting spherical cage does not provide an acceptable model for a Fullerene, and a full density functional theory treatment with the intent of obtaining an effective valence electron interaction potential is exceedingly difficult. So, in many cases, a "jellium-shell" model is employed in order to simulate the attraction of an electron with the cage, which involves a spherical step function potential well. Such models have been utilized to calculate the photoabsorption spectrum of C_{60} as well as that for endohedral Xe and Ba [7]. In addition, the jellium-shell model has been used to reproduce certain aspects of the photoionization cross section of C_{60} [8] and it has been successfully applied to other endohedral Fullerene systems [9-11].

With the recent surge in knowledge about novel nanoscale devices there is currently intense scientific interest in a variety of confining systems to which both relativistic and non-relativistic quantum mechanical formalisms may be applied with varying degrees of success [12] as well as in molecular species confined within Fullerenes [13]. However, some relevant recent works on confined hydrogen - the most simple system to study theoretically - nicely compliment the earliest papers [4,5]. For example, variational perturbation theory is used to study the positional behavior of confined H [14] and a numerical solution to Schrödinger's Equation is employed to examine the behavior of confined H which is isotropically compressed [15]. In the interest of better understanding the behavior of species encapsulated within Fullerenes, a jellium shell model has been used in a recent study of the behavior of H confined at the center of a deformable cage [16], showing outstanding agreement with experiment and other theoretical results.

Interestingly, results of various investigations suggest that the encapsulated species might reside off-center [13], especially in the case where the confining cage is attractive, but not repulsive. Since the studies of confined and encapsulated hydrogen are of great interest, it is beneficial to generalize the existing model to any encapsulated system with the effective atomic/ionic nucleus placed at some arbitrary position within the encapsulating shell. The purpose of the work presented here is to calculate the spectral behavior of on-center as well as off-center hydrogenic species (with one valence electron) in a spherical jellium-shell. Particular emphasis is placed on $H@C_{60}$ and $Mg^{+}@C_{60}$ in order to not only provide comparisons and contrasts with existing work on the relatively well-explored encapsulated hydrogen system, but to also utilize the computational method for the relatively new terrain of encapsulated magnesium, as recent experimental optical and mass spectroscopic studies of magnesium-Fullerene systems show a small fraction of endohedral complex formation [17].

Computational Approach

i. On-center calculations

The Schrödinger Equation describing the quantum mechanical wave function for a particle is

$$-\frac{\hbar}{2m}\nabla^2\Psi_{n\ell m}(\vec{r})+V(\vec{r})\Psi_{n\ell m}(\vec{r})=E_{n\ell m}\Psi_{n\ell m}(\vec{r}). \quad (1)$$

When using atomic units Equation (1) becomes much more convenient to work with as $\hbar$ and m are both equal to unity. We then obtain

$$-\frac{1}{2}\nabla^2\Psi_{n\ell m}(\vec{r})+V(\vec{r})\Psi_{n\ell m}(\vec{r})=E_{n\ell m}\Psi_{n\ell m}(\vec{r}). \quad (2)$$

In spherical geometry and with the atomic nucleus located at the center of the confining cage the electronic potential is dependent on only r. Since the angular parts $Y_\ell^m(\theta,\phi)$ of the wave function $\Psi(\vec{r})=A_{n\ell m}R_{n\ell}(r)Y_\ell^m(\theta,\phi)$ are well known, we become interested in obtaining the radial part of the wave function, and Equation (2) becomes

$$-\frac{1}{2}\left\{\frac{1}{r^2}\frac{d}{dr}\left(r^2\frac{d}{dr}\right)\right\}R_{n\ell}(r)+\frac{\ell(\ell+1)}{r^2}R_{n\ell}(r)+V(r)R_{nl}(r)=E_{n\ell}R_{n\ell}(r). \quad (3)$$

The reduction of Equation (2) to a one-dimensional form significantly reduces the computational time and memory demands, allowing for a considerable increase in precision for the calculations to be conducted.

The electron experiences two interactions: one with the nuclear core, $V_{core}(r)$, and the other with the jellium-shell, $V_{shell}(r)$; thus $V(r)=V_{core}(r)+V_{shell}(r)$ in Equation (3). The valence electron-core interaction has the form [18]

$$V_{core}(r)=\frac{-\gamma}{r}+\frac{\alpha}{r}e^{-\beta r}. \quad (4)$$

V_{core} represents the potential for the outermost electron in Mg^+, and is calculated using density functional theory. Hence, Mg^+ is referred to as being *hydrogenic*. The potential shown in equation 4 is purely Coulombic for H and parameters α,β and γ for both species are given in Table I.

Table I. Parameters for the hydrogen and magnesium valence electron potentials calculated utilizing density functional theory [18] as well as those for the cage, which is modeled using a standard jellium shell formalism[8-11,16]. Note that, for hydrogen, β may be any real number. All values are in atomic units unless otherwise indicated.

Parameter	**Value**
α	0 (H) 20.657 (Mg^+)
β	0 (H) 2.55 0(Mg^+)
γ	1.000 (H) 2.000(Mg^+)
U_o	-0.302
R_s (Å)	3.04
Δr (Å)	1.00

The encapsulating ("confining") cage is approximated as a spherical square well [8-11, 16] and has the functional form

$$V_{shell}(r) = \begin{cases} 0, & r < R_s - \Delta r \\ U_0, & R_s - \Delta r \le r \le R_s + \Delta r, \\ 0, & r > R_s + \Delta r \end{cases} \qquad (5)$$

where the parameters U_0,R_s and Δr are also given in Table I. The square well is negative (U_0<0) because the cage has empty states that the valence electron can occupy and is therefore effectively attractive. The well depth is adjusted so that the model reproduces the electronic behavior of a single electron in the jellium shell as calculated from first principles [8] or the photoionization behavior of other caged species.[9-11, 16] We chose the latter parameters due to the similarity of the models involved.

Now Equation (3) must be discretized in order to pursue a numerical solution. The finite-difference method selected is similar to those used to solve the time-independent Schrödinger Equation in Cartesian coordinates [19] and for time-dependent eigenvalue problems having cylindrical symmetry [20]. A necessary requirement in the model is a non-interacting impenetrable spherical barrier. Therefore, the atom and Fullerene are placed in a spherical cavity of radius R with an infinite potential beyond the container, which allows calculations to be executed over the finite volume of the container. Although a necessary computational tool, the hard spherical shell boundary is constructed so that it is sufficiently large so as to have a negligible effect on results central to this work. To simplify the form of Equation (3) the transformation $u_{n\ell}(r) = rR_{n\ell}(r)$ is made. Requiring $\Psi(R) = 0$ per the hard sphere boundary conditions, as well as $|\Psi(0)| < \infty$ the following boundary value problem is obtained:

$$\frac{d^2 u_{n\ell}(r)}{dr^2} - 2V(r)u_{n\ell}(r) - 2\frac{\ell(\ell+1)}{r^2}u_{nl}(r) = -2E_{n\ell}u_{n\ell}(r); \quad (6a)$$

$$u_{n\ell}(0) = u_{n\ell}(R) = 0. \quad (6b)$$

Space is divided into finite one-dimensional elements of width Δr. Subsequent discretization of the derivative in Equation (6) results in

$$\frac{u_{i+1} - 2u_i + u_{i-1}}{\Delta r^2} - 2V(r_i)u_i - 2\frac{\ell(\ell+1)}{r_i^2}u_i = -2E_{nl}u_i, \quad (7)$$

for i=1,2,3,…,N, with $u_i = u_{n\ell}(r_i)$.

We now have N simultaneous eigenvalue equations for each radial element index (i) and these equations may be cast in the following form:

$$\begin{bmatrix} B_1 & A & 0 & 0 & \cdots & 0 \\ A & B_2 & A & 0 & \cdots & 0 \\ 0 & A & B_3 & A & \cdots & 0 \\ 0 & 0 & A & B_4 & \cdots & 0 \\ \vdots & \vdots & \vdots & \vdots & \cdots & \vdots \\ 0 & 0 & 0 & 0 & \cdots & B_N \end{bmatrix} \begin{bmatrix} u_1 \\ u_2 \\ u_3 \\ u_4 \\ \vdots \\ u_N \end{bmatrix} = E_{nl} \begin{bmatrix} u_1 \\ u_2 \\ u_3 \\ u_4 \\ \vdots \\ u_N \end{bmatrix}, \qquad (8)$$

where $A = \frac{1}{\Delta r^2}$ and $B_i = \frac{-2}{\Delta r^2} - 2V(r_i)$.

The eigenvalue problem (8) is now solved using a routine in matrix library, giving both the energy of the atom or ion and its wave function.

ii. Off-center calculations

Since the results of many studies suggest that an encapsulated species may not reside at the geometrical center of the confining cage, off-center calculations are of interest. When studying the effect of moving the atom off-center, the resulting dimensionality increase in the Schrödinger equation adds considerable challenges for both computational time and memory. Therefore to keep the resulting equation two-dimensional the nucleus is placed at a location $\vec{a} = a\hat{z}$, so as to preserve azimuthal symmetry. The resulting two-dimensional Schrödinger equation is

$$-\frac{1}{2}\left\{\frac{1}{r^2\sin\theta}\frac{d}{dr}\left(r^2\frac{d}{dr}\right)+\frac{1}{\sin\theta}\frac{\partial}{\partial\theta}\left(\sin\theta\frac{\partial}{\partial\theta}\right)-\frac{m^2}{\sin^2\theta}\right\}\psi_{n\ell m}(r,\theta)$$
$$+V(r,\theta)\psi_{n\ell m}(r,\theta)=E_{n\ell}\psi_{n\ell m}(r,\theta), \quad (9)$$

with the potential $V(r,\theta)=V_{core}(|\vec{r}-\vec{a}|)+V_{shell}(r)$ and subject to the boundary conditions $\psi_{n\ell m}(R,\theta)=0$ and $|\psi_{n\ell m}(R=0)|<\infty$. In a similar manner to that for the 1D case, equation (9) may be transformed to

$$\frac{\partial^2 F}{\partial r^2}+\frac{1}{r^2}\left(\frac{\partial^2 F}{\partial\theta^2}-\cot\theta\frac{\partial F}{\partial\theta}+\frac{F}{\sin^2\theta}\right)-\frac{m^2}{r^2\sin^2\theta}F-2V(r,\theta)F=-2E_{n\ell m}F, \quad (10)$$

with $F=F_{n\ell m}(r,\theta)=r\sin\theta\psi_{n\ell m}(r,\theta)$ subject to the transformed boundary conditions

$$F(0,\theta)=F(R,\theta)=F(r,0)=F(r,\pi)=0.$$

Space is then divided into area elements and a finite difference equation is obtained in a fashion similar to the one-dimensional case:

$$\frac{F_{i+i'}-2F_i+F_{i-i'}}{(\Delta r)^2}+\frac{1}{r_i^2}\left(\frac{F_{i+i''}-2F_i+F_{i-i''}}{(\Delta\theta)^2}-\cot\theta_i\frac{F_{i+i''}-F_{i-i''}}{2\Delta\theta}+\frac{F_i}{\sin^2\theta_i}\right)$$
$$-\frac{m^2}{r_i^2\sin^2\theta_i}F_i-2V(r_i,\theta_i)F_i=-2E_{n\ell m}F_i. \quad (11)$$

Here only one index is needed because the volume elements are numbered in sequence starting with i=0 in the middle of the sphere. The integers (i') and (i'') in Equation (11) are chosen in the radial and colatitudinal directions, respectively, so the correct derivatives are calculated and the proper boundary conditions are realized. Equation (11) is then cast in a form similar to Equation (8), and solved in the same way. The computational time and memory requirements for the two dimensional case are significantly greater than those for the one-dimensional case, mainly because the memory required for the one-dimensional simulations depends only on the number of radial grid points, while that for the two-dimensional simulations depends on the number of radial and colatitudinal grid points.

Discussion and Conclusions

Before discussing important aspects of the results of this work it is worthwhile to mention how the electronic states for the various species are labeled. In the case of H, the calculated states correspond exactly to the physical atomic states. In the case of Mg^+, however, the physical ground state

configuration begins at 3s, while the calculated ground state for its pseudo-hydrogenic model begins at 1s. This occurs because the model involving the pseudopotential ignores detailed electronic structure of the core and effectively washes out some of the radial wavefunction nodes. Therefore the node counter for the pseudo-hydrogenic model is reset at n=1 for the ground state. The result is a re-labeling of the pseudo-hydrogenic s and p states, as summarized in Table II. The remainder of the discussion refers to the *calculated* Mg^+ states with their *physical* labels clarifying, for example, why the *calculated* 3s state has no nodes while the *physical* 3s state has n-l-1=2 nodes; it is really a pseudo-hydrogenic 1s state.

Table II. Mg^+ electronic states and their corresponding pseudo-hydrogenic states.

Mg^+ State	**Pseudo-Hydrogenic State**
3s	1s
3p	2p
3d	3d
4s	2s
4p	3p
4d	4d
4f	4f
5s	3s
5p	4p
5d	5d
5f	5f
5g	5g
6s	4s
6p	5p
6d	6d
6f	6f
6g	6g
6h	6h
7s	5s
7p	6p
7d	7d
7f	7f
7g	7g
7h	7h
8s	6s
8p	7p
9s	7s

For validation of the computational method presented and valence electron interaction potentials used, species not confined within a Fullerene cage (free species) are first considered. Such simulations entail placement of the atom or ion at the center of the hard spherical shell without the jellium potential present. The radius of the shell is chosen to be R=50Å and there are N=3000 radial divisions. The spectra and energy levels of unconfined Mg^+ and H are well known; accepted values as well as our calculated values for several energy levels for both species are shown in Table III.

Table III. Accepted and our calculated values for selected energy levels of H [21] and Mg^+ [22]. Due to the computational algorithm the series calculated for the $n \geq 7$ states are incomplete. All values are in eV and are calculated so the free electron has energy E=0. States do not correspond across rows.

H State	H Accepted	H calculated in this work	Mg^+ State	Mg^+ Accepted	Mg^+ calculated in this work
1s	-13.6057	-13.6039	**3s**	-15.03527	-15.03539
			3p	-10.612838	-10.61292
2s	-3.40125	-3.40131	**3d**	-6.171505	-6.17166
2p	-3.40125	-3.40146			
			4s	-6.380556	-6.38061
3s	-1.51174	-1.51172	**4p**	-5.039722	-5.03976
3p	-1.51174	-1.51176	**4d**	-3.46617	-3.46626
3d	-1.51174	-1.51175	**4f**	-3.40572	-3.40562
4s	-0.85035	-0.85035	**5s**	-3.53071	-3.53074
4p	-0.85035	-0.85037	**5p**	-2.95238	-2.9524
4d	-0.85035	-0.85036	**5d**	-2.21282	-2.21288
4f	-0.85035	-0.85036	**5f**	-2.17949	-2.17938
			5g	-2.17753	-2.17742
5s	-0.54423	-0.54422			
5p	-0.54423	-0.54423	**6s**	-2.2405	-2.24052
5d	-0.54423	-0.54423	**6p**	-1.93977	-1.93978
5f	-0.54423	-0.54423	**6d**	-1.53337	-1.5334
5g	-0.54423	-0.54423	**6f**	-1.51339	-1.51328
			6g	-1.51218	-1.51207
6s	-0.37794	-0.37653	**6h**	-1.51182	-1.51183
6p	-0.37794	-0.37675			
6d	-0.37794	-0.3771	**7s**	-1.54773	-1.54774
6f	-0.37794	-0.37747	**7p**	-1.37177	-1.37178
6g	-0.37794	-0.37776	**7d**	-1.12459	-1.12462
6h	-0.37794	-0.37799	**7f**	-1.11178	-1.11167
			7g	-1.11100	-1.11089

Table III. Cont.

7s	-0.27766	-0.25009	**7h**	-1.11072	-1.11073
7p	-0.27766	-0.2525			
7d	-0.27766	-0.2569	**8s**	-1.13314	-1.13303
7f	-0.27766	-0.26252	**8p**	-1.0213	-1.0213
7g	-0.27766	-0.26835			
7h	-0.27766	-0.27774	**9s**	-0.86519	-0.86519

The values obtained from the simulation generally have excellent agreement with the accepted ones [21], and the patterns of variation from experimental results can give considerable insight into the workings and limitations of our model. The degeneracy in hydrogen is split by the large spherical hard shell because various angular momentum states with differing symmetry are affected uniquely by the boundary conditions imposed on the hard spherical shell. Such results agree well with the much more pronounced selective alterations of various wave functions under the influence of the deformable, prolate-ellipsoidal confining cage of Connerade and co-workers [16]. Likewise, those states corresponding to higher electronic probability densities at larger distances from the origin are affected more profoundly by a spherical cutoff. Magnesium energy levels are naturally non-degenerate in ℓ but its calculated spectrum has a higher percent error than does hydrogen because the magnesium has a broader wave function that doesn't go to zero so fast as hydrogen's does at the shell boundary. Such considerations also explain why higher energy levels have larger percent errors than the smaller ones for a given species. Overall, inspection of the data in Table III suggests that the calculation method and model used are reasonable, and that the hard spherical shell does not adversely affect the results in a considerable way. Moreover, the valence electron pseudo-potential used for the magnesium ion gives excellent agreement with experiment and therefore seems to be very reasonable over a wide range of energy levels.

The next set of calculations involves modeling endohedral species, so the jellium potential is introduced. Table IV shows our calculated encapsulated hydrogen and magnesium energy levels, along with those for encapsulated hydrogen obtained from an analytical treatment of a jellium-shell model by Connerade [16].

Table IV. Our calculated values for selected energy levels in H and Mg^+ in the jellium-shell cage, along with those for H calculated by Connerade *et al.* [16]. All energies are in eV and calculated so that the free electron has energy *E=0*. States do not correspond across rows.

H State	**Calculated (Endohedral H) Connerade *et al.* [16]**	**Calculated (Endohedral H) this work**	**Mg^+ State**	**Calculated (Endohedral Mg^+) this work**
1s	-13.616	-13.6143	**3s**	-15.2064
			3p	-11.5874
2s	-6.78244	-6.78127	**3d**	-9.10792

Table IV. Cont.

2p	-6.28502	-6.28401		
			4s	-10.2391
3s	-1.57282	-1.57318	**4p**	-7.94433
3p	-1.6803	-1.68037	**4d**	-6.87706
3d	-4.73846	-4.73729	**4f**	-3.51847
4s	-0.88192	-0.88206	**5s**	-3.7327
4p	-1.04016	-1.04026	**5p**	-3.29791
4d	-1.05907	-1.05912	**5d**	-4.39126
4f	-2.83312	-2.83367	**5f**	-2.48727
			5g	-2.41528
5s	-0.56613	-0.56621		
5p	-0.65131	-0.65141	**6s**	-2.34147
5d	-0.62804	-0.62793	**6p**	-2.06313
5f	-0.76556	-0.76555	**6d**	-1.85264
5g	-0.72233	-0.7233	**6f**	-1.9166
			6g	-1.63594
6s		-0.39234	**6h**	-1.67474
6p		-0.43927		
6d		-0.42076	**7s**	-1.61911
6f		-0.48961	**7p**	-1.43158
6g		-0.50989	**7d**	-1.38456
6h		-0.37796	**7f**	-1.32519
			7g	-1.74139
7s		-0.26773	**7h**	-1.21262
7p		-0.3069		
7d		-0.29267	**8s**	-1.161911
7f		-0.34121	**8p**	-1.0555
7g		-0.35716		
7h		-0.2734	**9s**	-0.90325

In addition, Figures 1 and 2 show comparisons of the energy levels with and without encapsulation for hydrogen and magnesium, respectively, and Figures 3 and 4 show selected radial wave functions $rR_{n\ell}(r)$ for the same systems.

Figure 1. Comparison of free and encapsulated ("confined") hydrogen energy levels in eV for n=1-7 as calculated in our work. Results are grouped by principal quantum number n and are arranged within each group by increasing angular momentum quantum number ℓ. Free hydrogen energies are in black and those for encapsulated hydrogen are in gray.

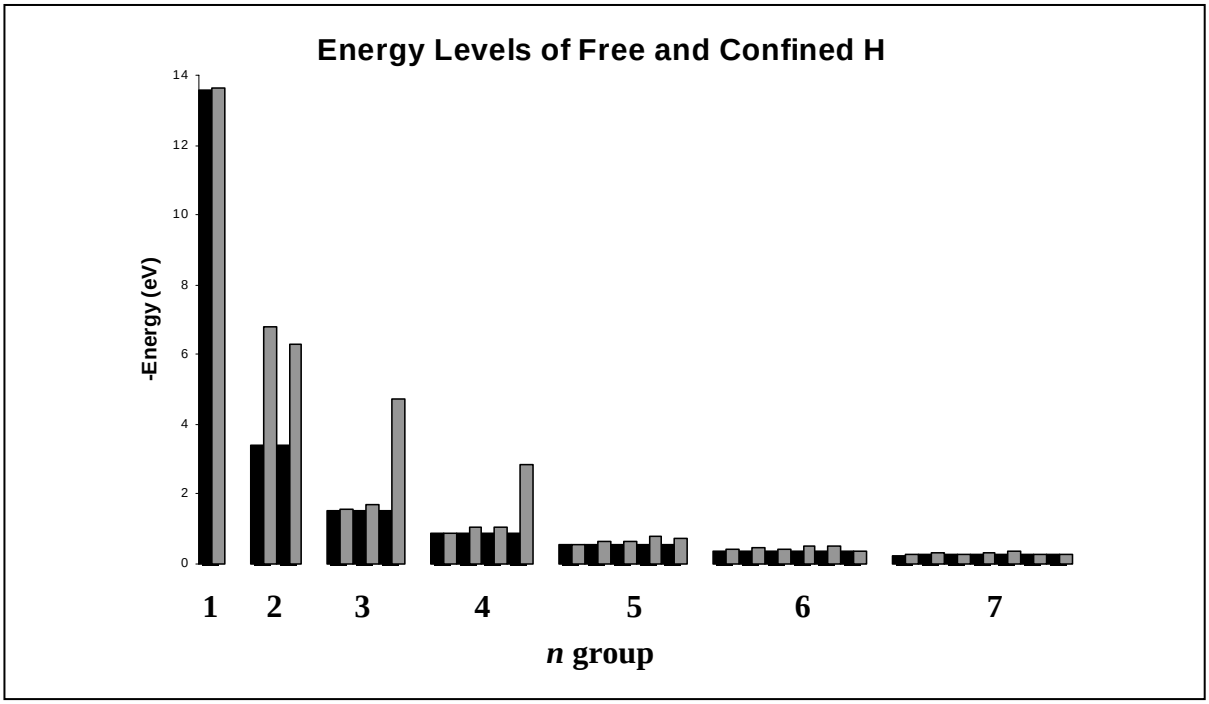

Figure 2. Comparison of energy levels in eV for free and encapsulated magnesium as calculated in our work. Format is the same as in Figure 1.

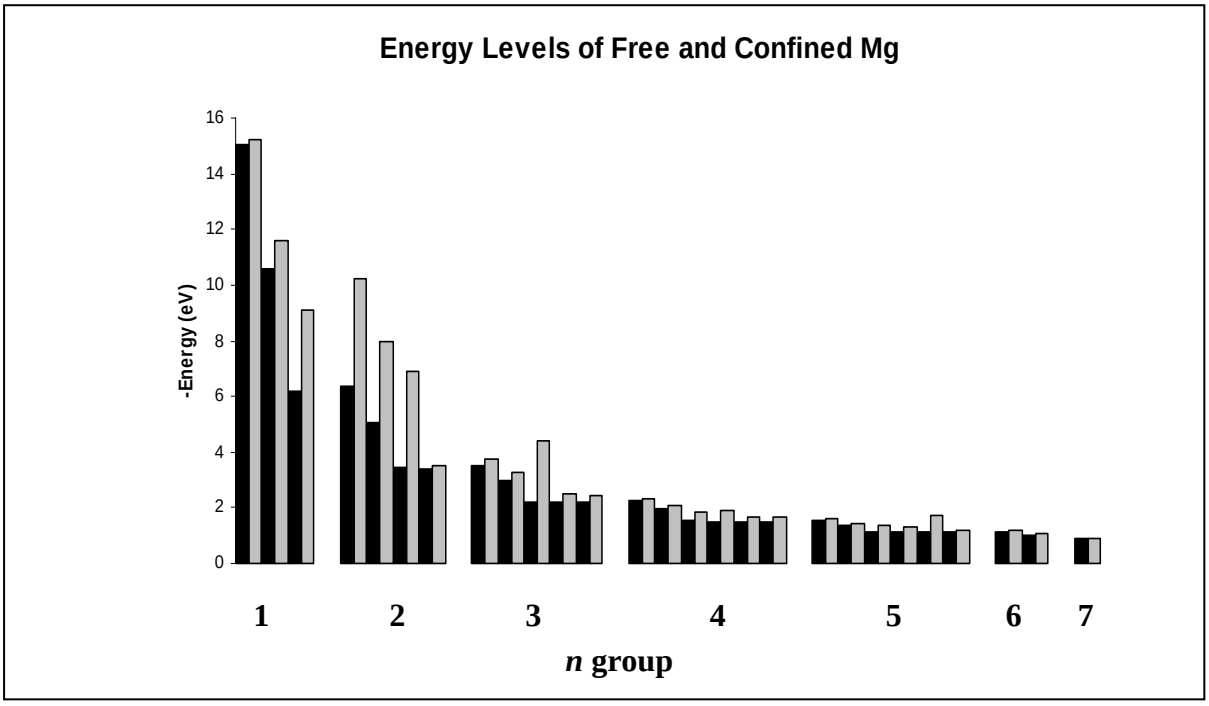

Figure 3. Radial wave functions $rR_{n\ell}(r)$ of free and encapsulated hydrogen for n=1-3. Results for the former are in black and for the latter in gray. The horizontal axis is distance from the nucleus in Angstroms and the vertical axes are arbitrary but identical for both encapsulated and free species for a given quantum state. The boundaries of the jellium-shell are represented by vertical black lines. Various pairs of states are normalized and offset by different vertical amounts for visual clarity, and dashed horizontal lines within the jellium boundary indicate the respective wave function zeroes.

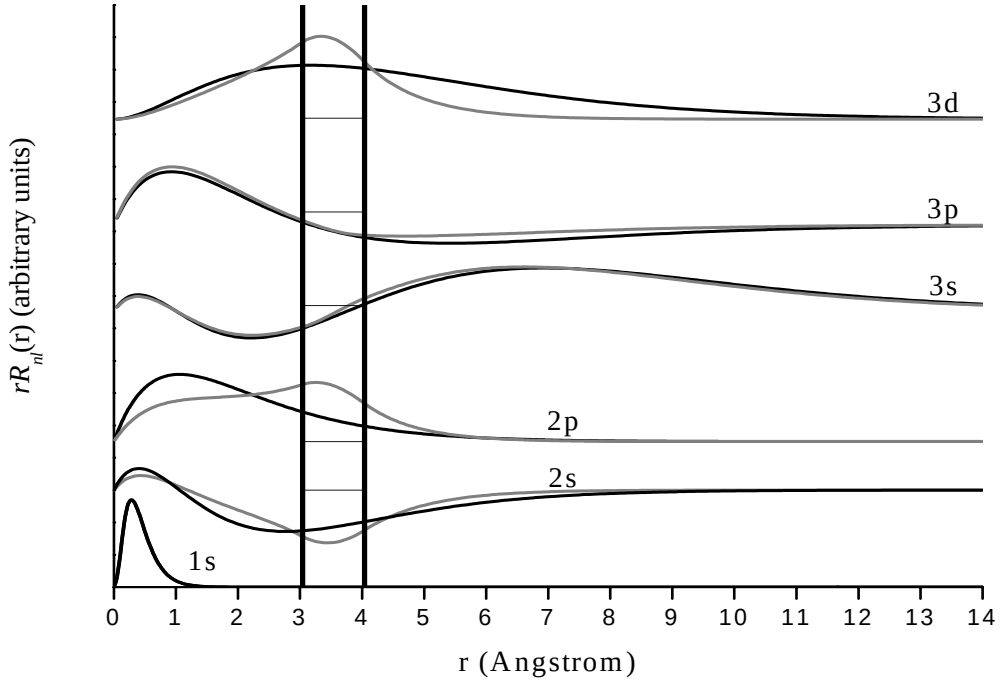

Figure 4. Radial wave functions $rR_{n\ell}(r)$ of free and encapsulated magnesium for states corresponding to those for hydrogen in Figure 3. Format is the same as in Figure 3 but vertical scales do not correspond.

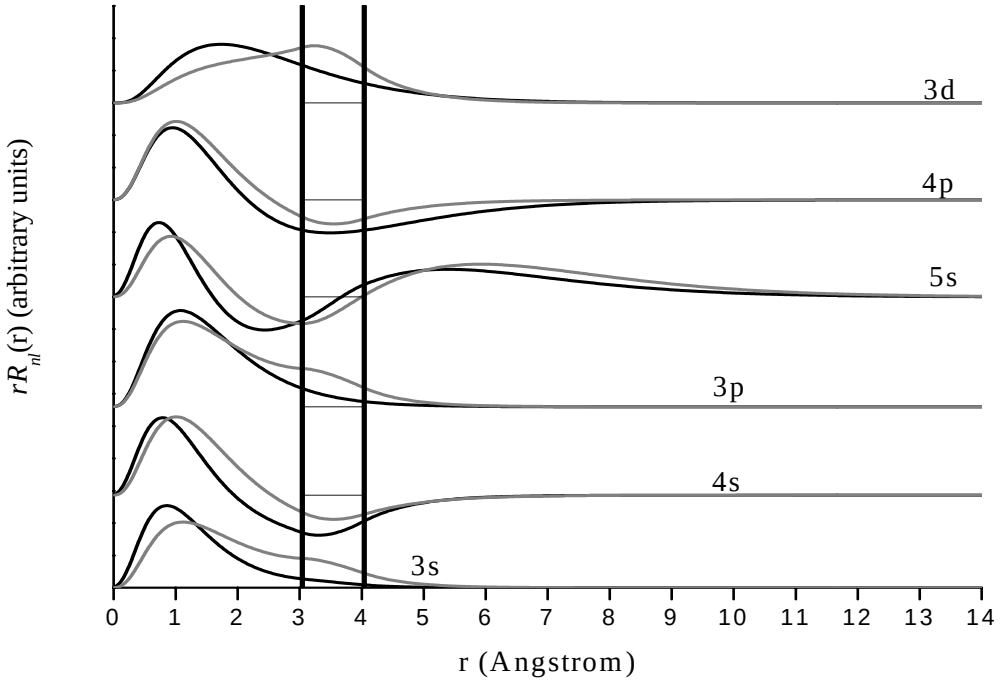

Our results for encapsulated H agree well with Connerade's, suggesting that the jellium-shell model utilized in this study yields reasonable results in the context of other similar models. Most of the hydrogen energy levels are altered only slightly by encapsulation, with the exception of some of those corresponding to higher *n* and highest angular momentum (ℓ) states within a given *n* level. Inspection of the wave functions shows that the energy levels are altered considerably in two types of situations. The first case includes those states where the electron probability density for the free species is near a maximum inside the jellium-shell. Examples are the 2s and 3d states. Such a consideration makes obvious sense because the jellium-shell is affecting the electron in a region of space where it would tend to spend most of its time. The second case is when the free species electron probability density is not near a maximum inside the cage but the shell *induces* a *global* maximum electron probability density inside it. Examples include the 2p state, and the corresponding physical interpretation is that the attractive cage is causing the electron to spend most of its time where the confining potential can affect it. The 1s state practically vanishes throughout the cage radius, so the corresponding wave function and energy level are virtually unaffected by confinement. The same is true for other states having a zero within or near the cage.

The behavior of magnesium is quite similar to that of hydrogen, with an interesting difference. Since the 3s wave function of magnesium vanishes much more slowly with increasing *r* than does the corresponding (1s) state for hydrogen, it does not vanish within the cage so encapsulation does have an effect on that state for magnesium. However there is neither a probability density maximum near the cage nor does the cage induce a *global* maximum in probability density within it. Hence, even though the cage deforms the wave function and induces a larger probability density within the cage than is present in the free species, the 1s energy level is still almost unaffected by its presence. Other examples are the 3p and 5s states. We emphasize that for Mg^+ one must be very careful with interpretation of the results because of the re-labeling of the s and p states discussed earlier. We suspect that the results for encapsulation have physical significance due to the close agreement of the free Mg^+ calculations and the accepted energy levels. However, it could be that the presence of more nodes in the physical s and p states than in the corresponding pseudo-hydrogenic states may have some effect on spectral changes in the encapsulated species, especially when there are nodes or anti-nodes of the wave function within the jellium shell.

The calculations for the off-center hydrogen take considerable computational time and memory and are thus limited in scope. Investigations of off-center hydrogen reveal that the lowest energy for the system occurs when the hydrogen atom sits slightly off-center at around a=0.1 Å (2.8% of the cage radius) and has a value of around –14.01 eV. In addition there seems to be some undulation present in the ground state energy as the nuclear offset varies, which is not well understood. Preliminary off-center calculations suggest that p states have no off-center minima. Off-center calculations are not presented for magnesium because, due to the broadness of its wave functions, radial and colatitudinal partitioning yielding sufficient accuracy in calculation was not possible.

Acknowledgements

The second author acknowledges illuminating and insightful discussions with Siu Chin at TAMU who provided invaluable insight into the theoretical aspects of the problem. M.R. and H.S.

acknowledge partial support for this work from Texas Higher Education Coordination Board grant no. 010366-082 as well as from Welch Foundation grant A-1546. Moreover W.E. and J.S. gratefully acknowledge financial support from the University of Northern Iowa Physics Department Summer 2002 Research Fellowship Program.

References and Notes

1. Liboff**,** R.L. *Introductory Quantum Mechanics, Fourth Edition*; Addison Wesley: San Francisco, CA, **2003**.
2. Griffiths, D.J. *Quantum Mechanics*; Prentice Hall: Upper Saddle River, NJ, **1994**.
3. Townsend, J.S. *A Modern Approach to Quantum Mechanics*; University Science Books: Sausalito, CA, **2000**.
4. Michels, A.; de Boer, J.; Bijl, A. Remarks concerning molecular interaction and their influence on the polarizability. *Physica* **1937,** *4*, 981-994.
5. Sommerfeld, A.; Welker, H. Kunstliche Grenzbedingungen beim Keplerproblem. *Ann. Phys.* **1938**, *32*, 56-65.
6. Kroto, H.W.; Heath, J.R.; O'Brien, S.C.; Curl, R.F.; Smalley, R.E. C60 – Buckminsterfullerene. *Nature* **1985,** *318*, 6042, 162-163.
7. Puska, M.J.; Nieminen, R.M. Physisorption of atoms inside C_{60}. *Phys. Rev. A* **1993**, *47*, 2, 1181-1186.
8. Xu, Y.B.; Tan, M.Q.; Becker, U. Oscillations in the potoionization cross section of C_{60}. *Phys. Rev. Lett.* **1996**, *76*, 3538-3541.
9. Connerade, J.P., Dolmaov, V.K.; Manson, S.T. A Unique Situation for an Endohedral Metallofullerene. *J. Phys. B: At. Mol. Opt. Phys.* **1999**, *32*, L395-L404.
10. Connerade, J.P., Dolmaov, V.K. Lakshmi P.A.; Manson, S.T. Electron Structure of Endohedrally Confined Atoms: Atomic Hydrogen in an Attractive Shell. *J. Phys. B: At. Mol. Opt. Phys.* **1999**, *32*, L239-L245.
11. Connerade J.P.; Semaoune. R. Relativistic study of the electronic structure and 5d orbital of La confined inside a C_{60} fullerene cage. *J. Phys. B: At. Mol. Opt. Phys.* **2000**, *33*, 869-880.
12. Connerade, J.P.; Kengkan, P.; Semaoune, R. Confined Atoms in Clusters Bubbles Dots and Fullerenes. *J. Chin. Chem. Soc.* **2001**, *48***,** 265-274, and references contained therein.
13. Krause M.; Hulman M.; Kuzmany H.; Dennis T.J.; Inakuma M.; Shinohara, J. Diatomic metal encapsulates in Fullerene cages: A Raman and infrared analysis of C84 and Sc2@C84 with D2d symmetry. *Chem. Phys.* **1999**, *111*, 17, 7976-7984.
14. Montgomery. H. E. Variational Perturbation Theory of the Confined Hydrogen Atom. *Int. J. Mol. Sci.* **2001**, *2*, 103-108.
15. Goldman, S.; Joslin, C. Spectroscopic properties of an isotropically compressed hydrogen atom. *J. Phys. Chem.* **1992**, *96*, 6021-6027.
16. Connerade, J.P.; Lyalin, A.G.; Semaoune, R.; Semenov, S.K.; Solov'yov, A.V. A simple atomic model for hydrogen confined inside a prolate-shaped C60 fullerene cage. *J. Phys. B: At. Mol. Opt. Phys.* **2001**, *34***,** 2505-2511.

17. Thompson, R.I.; Welling, M.; Schuessler, H.A.; Walther, H. J. Gas Phase Trapped Ion Studies of Colisionally Formed $MgC60^{+}$ Complexes. *J. Chem. Phys.* **2002**, *116*, 23, 10201-10211.
18. Chin, S.A. Private communication.
19. Harker, J.C. Numerically Solving the Schrödinger Equation, manuscript, Marlboro College, VT, **2002**.
20. Carnahan, B; Luther, H.A.; Wilkes, J.O. *Applied Numerical Methods*; John Wiley and Sons, Inc.: New York/London/Sydney/Toronto, **1969**.
21. Martin W. C.; Zalubas, R. Energy Levels of Magnesium, Mg I through Mg XII. *J. Phys. Chem. Ref. Data* **1980**, *9*, 1.
22. NIST Atomic Spectra Database Levels Form, http://physics.nist.gov/cgi-bin/AtData/levels_form?XXT1, last accessed November 13, 2004.

© 2004 by MDPI (http://www.mdpi.org).